Analysis of Sensing Mechanisms in a Gold-Decorated SWNT Network DNA Biosensor

Jinhong Ahn[1], Seok Hyang Kim[2], Jaeheung Lim[2], Jung Woo Ko[3], Chan Hyeong Park[4], and Young June Park[1, 2]

Abstract—**We show that carbon nanotube sensors with gold particles on the single-walled carbon nanotube (SWNT) network operate as Schottky barrier transistors, in which transistor action occurs primarily by varying the resistance of Au-SWNT junction rather than the channel conductance modulation. Transistor characteristics are calculated for the statistically simplified geometries, and the sensing mechanisms are analyzed by comparing the simulation results of the MOSFET model and Schottky junction model with the experimental data. We demonstrated that the semiconductor MOSFET effect cannot explain the experimental phenomena such as the very low limit of detection (LOD) and the logarithmic dependence of sensitivity to the DNA concentration. By building an asymmetric concentric-electrode model which consists of serially-connected segments of CNTFETs and Schottky diodes, we found that for a proper explanation of the experimental data, the work function shifts should be ~ 0.1 eV for 100 pM DNA concentration and ~ 0.4 eV for 100 μM.**

Index Terms—**Carbon nanotube, DNA sensor, Schottky barrier, work function, CNT network**

Manuscript received Aug. 22, 2013; accepted Mar. 8, 2014
[1] NANO Systems Institute (NSI), Seoul National University, Seoul 151-742, Korea
[2] Department of Electrical and Computer Engineering, Seoul National University, Seoul 151-742, Korea
[3] Technology Commercialization Division-SMEs Cooperation Center, ETRI, Daejeon 305-700, Korea
[4] Department of Electronics and Communications Engineering, Kwangwoon University, Seoul 139-701, Korea
E-mail : chanpark@kw.ac.kr

I. INTRODUCTION

Nano-biosensor technology, a convergence of biosensor and nano technologies has been emerged to be one of the most promising candidates to overcome the barriers of current biomedical issues such as single-molecule analysis, real-time detection, low-power consumption and miniaturization, to be used as in vivo applications [1, 2]. Among a number of approaches using various nanomaterials, single-walled carbon nanotubes (SWNTs) are the ultimate biosensor in this class for a couple of reasons: SWNTs have the smallest diameter (~ 1 nm), directly comparable to the size of single biomolecules. Furthermore, the one-dimensional (1-D) structure of carbon nanotubes (CNTs) allows signals to be propagated in a confined 1-D space, making them extremely sensitive to electrical and chemical changes in their immediate environments.

A drawback of sensors using a single SWNT is that its electrical properties are hard to control. For example, the energy gap of a nanotube is dependent on the tube diameter and the chiral vector, which implies the very high variability of electrical properties. In addition, the lack of reliable solutions to incorporate the biomaterials to the SWNT surface poses another challenge. A variety of biological molecules have been reported that can be bonded to CNTs [3, 4]. However, this often alters the intrinsic structure and properties of CNTs as well as those of attached biomolecules.

Recently, a new CNT-based electrical DNA biosensor system was reported by our group, which consists of gold (Au) nanoparticle-decorated SWNT network on top of concentric Au electrodes [5]. The Carbon Nanotube

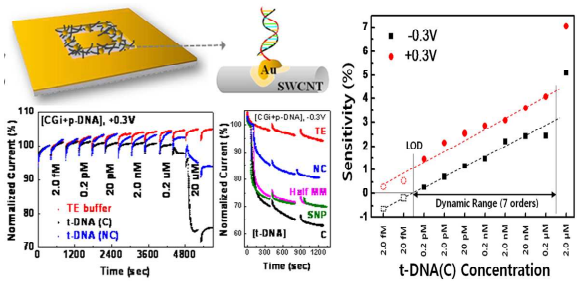

Fig. 1. DNA real-time measurement results and sensitivity curve using a gold-decorated SWNT network DNA Sensor [5].

Network Field-Effect Transistor (CNNFET) is made by using the SWNT network deposited on the concentric electrodes and in-between, to form an electrical channel of circular shape between the island electrode and the common enclosing one (see Figs. 1 and 2). Decorated Au nanoparticles on the SWNT network can be used as a platform or a linker for biomolecular sensor application by attaching probe molecules with thiol functional groups. They also provide better adhesion between the SWNT network and the chip substrate. Impressive features of this sensor include a very good sensitivity showing the limit of detection (LOD) of ~ 100 fM and a very wide dynamic range as large as seven orders of magnitude of target molecule concentration as shown in Fig. 1.

In Sec. II, an electrical model of the CNNFET is presented. Specifically, a serially-connected segment model for an asymmetric electrode structure is introduced. Transistor's current-voltage (*I-V*) characteristics are calculated for statistically-simplified geometries and compared with the measurement results. In Sec. III, to match the experimental and simulation results, a metal-Schottky junction model is incorporated into the serially-connected segment model. With this model, we show that carbon nanotube sensors with gold particles on the SWNT network operate as Schottky barrier transistors, in which a transistor action occurs primarily by varying the contact resistance of Au-SWNT junction rather than the channel conductance modulation as in a conventional MOSFET. Experimental and simulation results are discussed in Sec. IV and conclusions follow in Sec V.

II. Electrical Model of CNNFET

Changes in the conductivity of CNNFETs are mostly

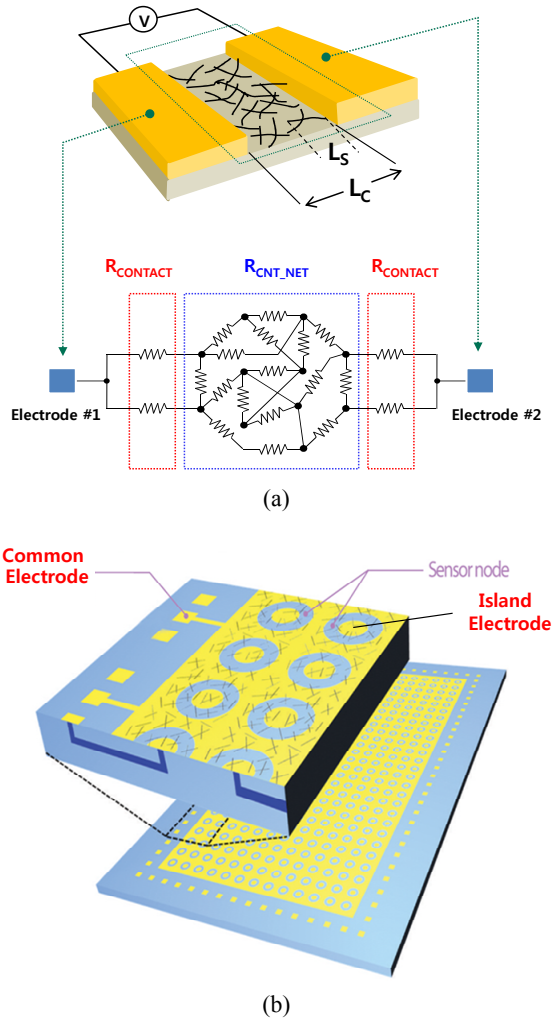

Fig. 2. Schematic of randomly-networked CNTs and the geometries of electrode formations (a) The networked CNT resistors with bar-type electrode configuration, (b) The networked CNT resistors with concentric-type electrode configuration.

due to the gate-coupling effect and the Schottky-barrier effect. To model the CNNFETs, we need to simplify the structures from both a physical and a statistical point of view. The basic structure of DNA sensor is the percolating network of randomly-oriented carbon nanotubes, as shown in Fig. 2. In the "short-channel" limit of $L_C < L_S$ (where L_C is the channel length and L_S the CNT stick length) and at low CNT density ρ_S, the CNTs behave as individual transistors connected in parallel bridging the source and drain electrodes. Therefore, the ratio of the transistor drain current I_D for any two bias points is independent of the geometry of the CNT networks. This implies that the scaling relationship can be written as,

$$I_{DS} = \frac{A}{L_S}\xi\left(\frac{L_S}{L_C}, \rho_S L_S^2\right) f\left(V_{GS,} V_{DS,}\right) \quad (1)$$

where the proportionality constant A depends on the gate capacitance C_{CNT} and the tube diameter d. ξ and f are functions of geometrical parameters L_C, L_S, and ρ_S and bias conditions (drain-to-source voltage V_{DS} and gate-to-source voltage V_{GS}), respectively [6, 7]. For long-channel CNTs with $L_C > L_S$ (see Fig. 2(a)), the individual CNTs cannot bridge the channel by themselves and the CNT-to-CNT interaction (C_{ij} between the i-th and j-th CNT) becomes important.

When calculated using ~ 200 statistical samples, the scaling formula of Eq. (1) still holds for arbitrary geometrical and biasing conditions even in the "long-channel limit" of $C_{ij} \neq 0$. Moreover, it was shown that the bias-dependent scaling function

$$f(V_{GS}, V_{DS}) = [(V_{GS} - V_{TH})V_{DS} - \beta V_{DS}^2] \quad (2)$$

is independent of geometrical parameters ($\beta \sim 0.5$), again satisfying Eq. (1) [7]. This means that the voltage scaling function $f(V_{GS}, V_{DS})$ would follow the classical square-law formula at very low densities ($\rho \ll \rho_{th}$ and $L_C < L_S$), and at very high densities ($\rho \gg \rho_{th}$) where ρ_{th} is the percolation threshold. After all, for $\rho \ll \rho_{th}$ and $L_C < L_S$, the CNT-to-CNT interaction is negligible, and the CNTs bridge the source and drain (S/D) directly, so that the system behaves as an independent collection of 1-D conductors. At $\rho \gg \rho_{th}$, the percolating network approximates a classical 2-D homogeneous thin film, and once again, the classical MOSFET formula should hold. These results imply that for any networked CNT sensor, only one CNNFET can model the current ratio of all the system.

A simplified diagram of the CNNFET is shown in Fig. 3. It consists of a networked CNT film as a semiconductor on top of an oxide as an insulator. Two metal contacts with the CNT film act as source and drain terminals. On top of the CNT film, there is a DNA membrane. For the biosensor application, the gate consists of a reference electrode and an electrolyte.

To solve the CNNFET's current equation, the Poisson-Boltzmann (PB) equations involving the charge and potential drop in the DNA membrane and bulk electrolyte are employed as follows.

The PB equations for the electrolyte region and DNA membrane region are given by [8, 9]

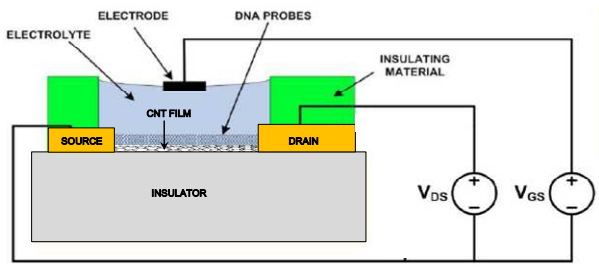

Fig. 3. Simplified diagram of the CNNFET for DNA sensor.

$$\frac{\partial^2 \psi}{\partial x^2} = \frac{2qzn_0}{\epsilon_{sol}} \sinh\left(z\beta\, \psi(x)\right) \quad (3a)$$

$$\frac{\partial^2 \psi}{\partial x^2} = \frac{2qzn_0}{\epsilon_m} \sinh\left(z\beta\, \psi(x)\right) - \frac{q\,\nu N_m}{\epsilon_m} \quad (3b)$$

where $\beta = q/kT$, ε_{sol} and ε_m are the electrical permittivity of the electrolyte and DNA membrane, where the electrolyte contains anions and cations with concentration n_0 and equal valence z (a z:z electrolyte). The membrane contains uniformly distributed fixed charges which have a valence ν and a concentration N_m. These equations can be solved to give the surface potential of the electrolyte, denoted by ψ_0.

Here, let us assume the CNT film as the conventional semiconductor bulk. The electrostatic potential drop within the semiconductor CNT is related to the total charge density through Poisson's equation, which, in 1-D, is given by

$$\frac{\partial^2 \psi}{\partial x^2} = -\frac{\rho(x)}{\epsilon_c} \quad (4)$$

where ε_c is the permittivity of the CNT film. Furthermore, the charge density of the semiconductor is composed of three parts: fixed ionized-impurity charges, minority-carrier charges, and majority-carrier charges. Thus, we can write:

$$\rho(\psi) = q(p(\psi) - n(\psi) - N_A) \quad (5)$$

The density of mobile carriers can be related to the electrostatic potential (band bending) by Boltzmann's statistics which applies in the non-degenerate case [10]:

$$p(\psi) = p_{\infty}\, e^{-\beta\psi},\ n(\psi) = n_{\infty}\, e^{\beta\psi} = p_{\infty}\, e^{\beta(\psi - 2\phi_F)} \quad (6)$$

where $\phi_F (= kT/q \log(N_A/n_i))$ is the Fermi potential of the semiconductor and p_{c0} and n_{c0} are the hole and electron concentration in the CNT bulk. Combining these three equations, we arrive at the Poisson–Boltzmann equation for the semiconductor's potential:

$$\frac{\partial^2 \psi}{\partial x^2} = -\frac{q}{\epsilon_c}\left(p_{c0}\, e^{-\beta\psi} - n_{c0}\, e^{\beta\psi} - N_A\right) \tag{7}$$

From this differential equation, the total charge density per unit area is given by [10]:

$$\sigma_s(\psi_s) = -\mathrm{sgn}(\psi_s)\sqrt{2\epsilon_c N_A kT} \times \sqrt{e^{-\beta\psi_s} + \beta\psi_s - 1 + e^{-2\beta\phi_F}\left(e^{\beta\psi_s} - \beta\psi_s - 1\right)} \tag{8}$$

To complete the electrolyte-semiconductor system, it is required to satisfy the Kirchhoff's voltage law and the Gauss law given by

$$V_{GC} = E^{M} + \frac{1}{q}\mu_e^{C} - \psi_0 + \chi^{Sol} - \chi^{C} + \psi_s \tag{9}$$

$$\epsilon_c \frac{\partial \psi_s}{\partial x} = -\epsilon_m \frac{\partial \psi_0}{\partial x} \tag{10}$$

where V_{GC} is the potential applied between the reference electrode and the CNT, $E^{M} = -\mu_e^{M}/q + (\phi^{M} - \phi^{sol})$, the reference electrode potential, χ^{Sol} and χ^{C} the surface dipole potential of the electrolyte solution and CNT, respectively and μ_e^{C} is the electron's chemical potential energy of the CNT.

To determine the C_g which acts as the gate capacitance of the CNNFET, we need to review the electrical double-layer (EDL) theory as follows.

Fig. 4 shows a charge distribution of CNT−electrolyte system under an applied external bias. This distribution can be modeled using the known Poisson–Boltzmann equation. The diffuse layer is known as the Gouy–Chapman layer. However, it was noticed that the original theory of Gouy–Chapman overestimates the interface charge, and therefore, the capacitance of high-concentration electrolytes. This was remedied by Stern, who realized that ions cannot approach the surface closer than their ionic radii. The distance of the closest approach is called the outer Helmholtz plane (OHP) as shown in Fig. 4.

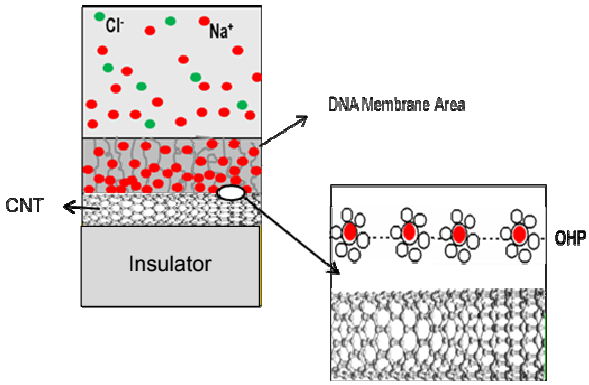

Fig. 4. Charge distribution of CNT−electrolyte system.

In the case that the DNA layer is treated as an ion-permeable membrane, the Donnan potential which is solely determined by the DNA concentration and the ion concentration of the electrolyte is formed. It is known that the Donnan potential is expressed as [8, 9]

$$\psi_{DP} = \frac{kT}{zq}\sinh^{-1}\left(\frac{\nu N_m}{2zn_0}\right) \tag{11}$$

Because the total net charge σ_{md} in the membrane and electrolyte is

$$\sigma_{m\,d} = -C_{DL}\left(\psi_0 - \psi_{DP}\right) \tag{12}$$

we can deduce the DNA-dependent double layer capacitance from a following equation:

$$\frac{1}{C_{DL}} = \frac{1}{C_{Stern}} + \frac{\lambda_m}{\epsilon_m\sqrt{\cosh\left(\frac{zq}{kT}\right)\psi_{DP}}} \tag{13}$$

where $\lambda_m = \sqrt{\dfrac{\varepsilon_m kT}{2n_0 z^2 q^2}}$ is the Debye length in the membrane. The gate capacitance C_g is modeled to be the double layer capacitance C_{DL}.

If we disregard the surface charge σ_f under an assumption that the CNT surface charge is small and does not change in time which is usually the case considering the inert surface characteristics of CNT to the electrolyte, we can solve all the equations in a self-consistent manner (using iterations), and the drain current can be calculated.

For the CNNFET with concentric electrodes which consists of the small island electrode and the common

enclosing electrode as shown in Fig. 2(b), there is another issue to be considered due to the asymmetrical nature of the biasing system. When this device is placed in an aqueous solution without the reference electrode for sensor applications, the electric potential of the liquid tends to follow the electric potential of the enclosing electrode due to the smaller redox resistance and larger electrical double layer capacitance between the liquid and the enclosing electrode. This different gate action to the carbon nanotube network channel results in an asymmetrical current profile depending on the voltage polarity.

When an electrolyte resistance is small, the use of the reference electrode using easily polarizable material, e.g. Ag/AgCl, can be used to remove this asymmetry. However, when the electrolyte resistance is high or real-time sensing is performed, the time-dependent current drift which occurs during the electrical double layer charge redistribution is inevitable. Therefore, we need to include this asymmetry in the modeling assuming the measurement is done in the steady-state after long wait time. Fig. 5 shows a schematic of a CNNFET with concentric electrodes which consists of n serially-connected transistor segments. Because the gate potential of each segment is determined by electrolyte resistances which can be calculated from the concentric disk problem, the previous single CNTFET equation can be applied to these small CNTFETs individually and the current flowing in the whole system can be obtained when the source and drain voltages of each small CNTFETs are determined by another iterations based on electrical circuit laws, e.g. Kirchhoff's laws.

Fig. 6 shows the comparison between actually measured and simulated DNA sensing results. The asymmetrical profile dependence on V_{DS} appears to be similar. However, several significant differences are found between the measured and simulated DNA sensing results. First of all, the current responses to DNA concentration are opposite. That is, as the concentration

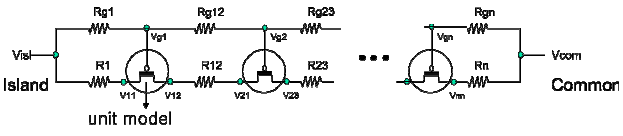

Fig. 5. Schematic of a CNNFET with concentric electrodes which consists of n serially-connected transistor segments.

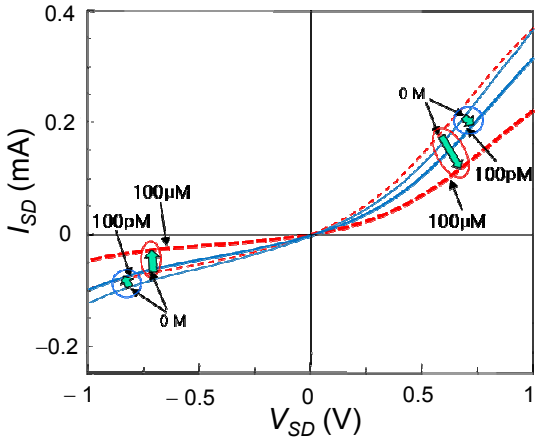

(a) Measured

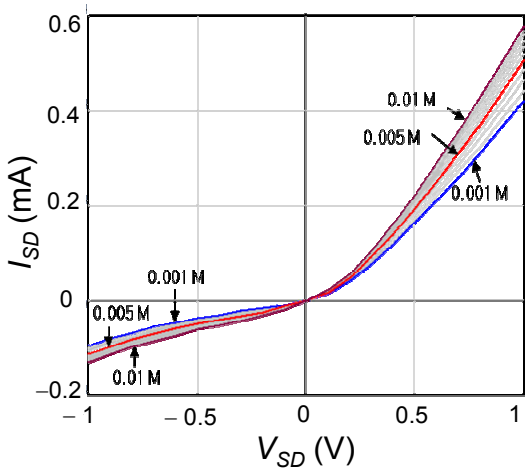

(b) Simulated

Fig. 6. Comparison between (a) measured, (b) simulated DNA sensing results.

of DNA increases, the measured current decreases as shown in Fig. 6(a), while the simulated current increases as in Fig. 6(b). The reason that the simulated current increases as the DNA concentration does can be explained as follows: a DNA sequence has negative charges because of the phosphate ions in its chemical backbone. In Eq. (3b), the negative charge of DNA is modeled by νqN_m where ν is equal to 1 and N_m is the density of charges in the membrane region and is a negative value for negative charge case. N_m is proportional to the DNA concentration (C_{DNA}) and can be expressed as $N_m = -K_a \cdot (N_{DNA} \cdot C_{DNA})$ where K_a is the surface adsorption factor which represents the ratio of surface DNA concentration to its bulk concentration. N_{DNA} is the number of negative charges contained in the one DNA molecule. In our CNNFET model, as the

magnitude $|N_m|$ of the negative charge density increases, the magnitude $|\psi_s|$ of the semiconductor surface potential increases. We modeled the change of CNNFET current using the strong inversion and charge-sheet models.

Secondly, the sensitivity to the DNA concentration is much better in the measured results than in the simulated ones. For example, the LOD of the measured results is less than 100 pM, while the LOD of the simulated ones is about 1 mM. Thirdly, the measured current shows the logarithmic response dependence on the DNA concentration, while the simulated current shows a linear response. These results clearly show that there is the other governing mechanism of CNT current flow which is different from the field-effect mechanism of CNTFET.

III. Electrical Model of Au-CNT Schottky Junction

To explain the Au-decorated CNNFET current phenomena which are different from the field-effect semiconductor theory, there have been a number of papers regarding metal-CNT interface effect, which explain the phenomena by a change of energy barrier height due to the shift of the energy alignment between the metal contact and CNT [11]. According to these reports, we can postulate that the modulation of the Schottky barrier height (SBH) at the metal-CNT contact by the efficient hybridization of DNA on metal electrodes is the dominant sensing mechanism. For the cause of the SBH change from the adjacent molecules in the electrolyte, it has been naturally assumed that this effect arises from the charge doping of the CNT surface [12, 13]. However, in the recent experiments for CNTs, it has been reported that the metal work function change is more plausible to the SBH change than the charge-doping effect is [14, 15].

In the absence of gate voltage, the hole carrier injection through the Schotty barrier formed at the metallic electrode/SWNT interface is dominated, at room temperature, by thermal emission. According to the theoretical descriptions of metal-semiconductor contacts by Schottky and Mott, the SBHs for electrons and hole are

$$\phi_{SBe} = \phi_m - \chi \tag{14a}$$

$$\phi_{SBh} = \chi + E_g - \phi_m \tag{14b}$$

where ϕ_m is the work function of the metal which is the energy needed to remove an electron from the Fermi level to the vacuum level and χ the electron affinity of the semiconductor which is the energy needed to remove an electron from the bottom of the conduction band to the vacuum level, and E_g is the band gap.

The current due to thermionic emission in a SB between two bulk materials is given by the ideal diode equation:

$$I = AA'T^2 e^{-\frac{\phi_{SB}}{kT}} e^{\frac{qV}{nkT}} \left(1 - e^{-\frac{qV}{kT}}\right) \tag{15}$$

where A is the contact area, $A' = 4\pi m^* q k^2/h^3$ the effective Richardson constant where m^* is the effective mass of the carrier, V the voltage applied to the semiconductor, T the temperature, n the ideality factor and $I_{sat} = AA'T^2 \exp(-\phi_{SB}/kT)$ the saturation current [16]. If $n > 1$, the current in the reverse direction increases exponentially with bias while the current for a forward bias is lowered compared to the ideal case. In this paper, however, we would like to focus the discussion only to the ideal case with $n = 1$ because we are interested in the change of work function itself, not the cause of work function change. If $n = 1$, there are no mechanisms that lowers the barrier and the current saturates at I_{sat} for a reverse bias larger than a few times kT/q since the reverse thermionic emission current injected into the metal from the semiconductor (first term in the parenthesis in Eq. (15)) vanishes. In the back-to-back Schottky diode model, the width of the depletion region is assumed so large that the tunneling current is negligible compared to the thermionic emission current. Further works may deal with non-ideal cases where the barrier height changes as the bias applies such as the image-force lowering of the SBHs under the reverse bias. If $n = 1$, Eq. (15) can be solved to extract the voltage drop existing in the Schottky junction, and the I_{SD} vs. V_{SD} characteristics of CNNFET can be described by the following analytical equation:

$$V_{SD} = R_f(V_{GS}) I_{SD} + \frac{kT}{q} \log\left(\frac{I_{sat} + I_{SD}}{I_{sat} - I_{SD}}\right) \tag{16}$$

where $R_f(V_{GS})$ is the resistance of CNNFET which is a function of V_{GS}. The first term on the RHS of Eq. (16) describes the linear part of the I_{SD} vs. V_{SD} curve due to

the CNNFETs, while the second one characterises the nonlinear part attributed to SBH.

IV. RESULTS AND DISCUSSION

To address the metal-CNT Schottky junction, back-to-back Schottky barrier diodes are employed. Because the gold particle size is larger than the CNT diameter, the interface between the CNT and the Au particle can be modeled as back-to-back Schottky diodes [17].

The gold nanoparticles are assumed to change the work function when the DNA hybridization occurs, causing the change of the Schottky barrier height (SBH) between the gold and the CNT. We disregarded the Schottky junction between the gold electrodes and the CNTs which are located on the Au electrodes because they are not the bottlenecks of the electrical current. Here it is noted that when the Schottky junction is formed at the interface between the Au electrode and the CNN channel, it can be a bottleneck as well as those between the gold nanoparticles and the CNTs in the CNN channel.

Fig. 7(a) shows a modified schematic of Fig. 5 which include back-to-back Schotty barrier diodes.

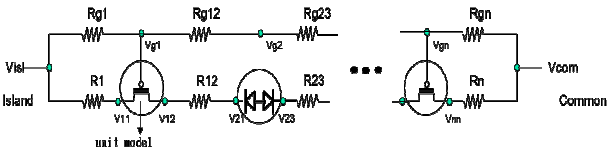

(a)

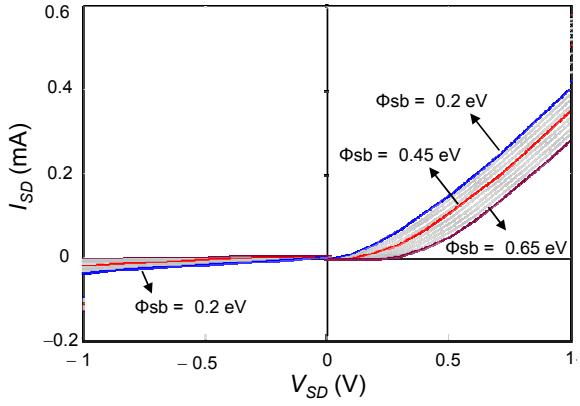

(b)

Fig. 7. Electrical model of Au-CNT and the simulation results (a) The schematic of a CNNFET with concentric electrodes where one of the segments is replaced by a back-to-back Schottky diode pair, (b) The simulated CNNFET current profile depending on the Schottky barrier height which comes from the work function modulation.

The device parameters used for this simulation are listed in Table 1. The simulated current profile shows that the current varies almost linearly as the Schottky barrier height changes, and the opposite response to the DNA concentration with the field effect transistor (CNTFET) model (Fig. 6(b)), can be resolved. In addition, we can calculate the work function change of DNA hybridization by comparing the experimental data and simulation results. By comparing Figs. 6(a) and 7(b), we can see that 100 pM DNA concentration gives about 0.1 eV work function change and 100 μM, about 0.4 eV work function change. From the measurement data and modeling, the work function shift is about 50 meV/decade of DNA concentration. The work function shifts show the logarithmic dependence of DNA concentration, and are in reasonable range when compared to the measurement data in the literature [18-20]. However, there are differences in Figs. 6(a) and 7(b) at the small voltage region and negative voltage region. In these regions, the current levels of Fig. 7(b) are very small and do not vary linearly according to the applied voltage bias, while Fig. 6(a) shows linear-like curves.

In the reverse voltage region, the field effect model looks better to fit the measured data when there are no DNA molecules. In the back-to-back Schottky model, in the reverse voltage region, it will be better for us to include the reverse current increase due to the Schottky barrier lowering by the image charge effect. But, in this paper, to show the main points and to reduce the complexity of the model, we did not include the reverse current increase effect.

Because a Schottky diode junction area is dependent on the CNT and gold particle densities, we should consider all possible current paths to be added for this parameter. In our simulation, the Schottky diode junction area is chosen to be 1 μm^2 as a fitting parameter.

Table 1. Device Parameters

Device Parameters	Simulation Values
Hole mobility of CNTFET	1000 cm^2/(V sec)
CNTFET channel length	10 μm
CNTFET channel width	10 μm
Schottky diode junction area	1 μm^2
Work function difference between Au and CNT	0.2 eV

V. CONCLUSIONS

By comparing the simulation results with the experimental data for the biosensor consisting of the SWNT FET network and the gold nanoparticles decorated on top of the CNT network, we suggest that the main origin of sensitivity is the work function shift of the gold, which changes the Schottky barrier height at the gold-CNT contact depending on the attached biomolecules. We demonstrated that the semiconductor MOSFET effect cannot explain the experimental phenomena such as the superb LOD and the logarithmic dependence of sensitivity to the DNA concentration. By building the asymmetric concentric-electrode model which consists of serially-connected segments of CNTFETs and back-to-back Schottky diodes, we found that the work function shifts are ~ 0.1eV for 100 pM DNA concentration and ~ 0.4eV for 100 μM DNA concentration.

ACKNOWLEDGMENTS

This work was supported by the Center for Integrated Smart Sensors funded by the Ministry of Science, ICT & Future Planning as Global Frontier Project (CISS-2012054186); and by the R&D Program of MKE/KEIT [10033590], Development of Disposable Cancer Diagnosis Sensor of Home-care Type with High Sensitivity; and by the Pioneer Research Center Program through the National Research Foundation of Korea funded by the Ministry of Science, ICT & Future Planning (NRF-2012-0009555); and by the Brain Korea 21 Plus Project in 2014. C. H. Park's research was supported by Basic Science Research Program through the National Research Foundation of Korea (NRF) funded by the Ministry of Education, Science and Technology (NRF-2012R1A1A2006893) and was supported by the Research Grant of Kwangwoon University in 2012.

REFERENCES

[1] J. Kong, N. R. Franklin, C. Zhou, M. G. Chapline, S. Peng, K. Cho, and H. Dai, "Nanotube molecular wires as chemical sensors," *Science*, vol. 287, pp. 622–625, 2000.

[2] K. Besteman, J. Lee, F. G. M. Wiertz, H. A. Heering, and C. Dekker, "Enzyme-coated carbon nanotubes as single-molecule biosensors," *Nano Lett.*, vol. 3, no. 6, pp. 727–730, 2003.

[3] A. Star, E. Tu, J. Niemann, J. P. Gabriel, C. S. Joiner, and C. Valcke, "Label-free detection of DNA hybridization using carbon nanotube network field-effect transistors," *Proc. Natl. Acad. Sci. U.S.A.*, vol. 103, no. 4, pp. 921–926, 2006.

[4] J. Wang, *Electroanalysis*, "Carbon-nanotube based electrochemical biosensors: A review," vol. 17, no. 1, pp. 7–14, 2005.

[5] J. W. Ko, J.-M. Woo, J. Ahn, J. H. Cheon, J. H. Lim, S. H. Kim, H. Chun, E. Kim and Y. J. Park, "Multi-order dynamic range DNA sensor using a gold decorated SWCNT random network," *ACS Nano*, vol. 5, no. 6, pp. 4365–4372, 2011.

[6] N. Pimparkar, J. Guo, and M. A. Alam, "Performance assessment of sub-percolating nanobundle network transistors by an analytical model," *IEDM Tech. Dig*., 2005, pp. 534–537.

[7] N. Pimparkar, Q. Cao, S. Kumar, J. Y. Murthy, J. Rogers, and M. A. Alam, "Current-voltage characteristics of long-channel nanobundle thin-film transistors: A "bottom-up" perspective," *IEEE Electron Device Lett*., vol. 28, no. 2, pp. 157–160, 2007.

[8] D. Landheer, G. Aers, W. R. McKinnon, M. J. Deen, and J. C. Ranuarez, "Model for the field effect from layers of biological macromolecules on the gates of metal-oxide-semiconductor transistors," *J. Appl. Phys.*, vo. 98, pp. 044701-1–15, 2005.

[9] D. Landheer, W. R. McKinnon, G. Aers, W. Jiang, M. J. Deen, and M. W. Shiwari, "Calculation of the response of field-effect transistors to charged biological molecules," *IEEE Sensors Journal*, vol. 7, no. 9, pp. 1233–1242, 2007.

[10] M. W. Shinwari, M. J. Deen, and D. Landheer, "Study of the electrolyte-insulator-semiconductor field-effect transistor (EISFET) with applications in biosensor design," *Microelectronics Reliability*, vol. 47, pp. 2025–2057, 2007.

[11] X. Tang, S. Bansaruntip, N. Nakayama, E. Yenilmez, Y.-l. Chang, and Q. Wang, "Carbon nanotube DNA sensor and sensing mechanism," *Nano Lett*., vol. 6, no. 8, pp. 1632–1636, 2006.

[12] S.-H. Jhi, S. G. Louie, and M. L. Cohen,

"Electronic properties of oxidized carbon nanotubes," *Phys. Rev. Lett*., vol. 85, no. 8, pp. 1710–1713, 2000.

[13] P. G. Collins, K. Bradley, M. Ishigami, and A. Zettl, "Extreme oxygen sensitivity of electronic properties of carbon nanotubes," *Science*, vol. 287, pp. 1801–1804, 2000.

[14] I. Heller, A. M. Janssens, J. Mannik, E. D. Minot, S. G. Lemay, and C. Dekker, "Identifying the mechanism of biosensing with carbon nanotube transistors," *Nano Lett*., vol. 8, no. 2, pp. 591–595, 2008.

[15] S. Heinze, J. Tersoff, R. Martel, V. Derycke, J. Appenzeller, and Ph. Avouris, "Carbon nanotubes as Schottky barrier transistors," *Phys. Rev. Lett*., vol. 89, pp. 106801-1–4, 2002.

[16] E. H. Rhoderick and R. H. Williams, *Metal-Semiconductor Contacts,* Clarendon Press, 2nd edition, 1988.

[17] M. S. Fuhrer, J. Nygård, L. Shih, M. Forero, Young-Gui Yoon, M. S. C. Mazzoni, Hyoung Joon Choi, Jisoon Ihm, Steven G. Louie, A. Zettl, and Paul L. McEuen, "Crossed Nanotube Junctions," *Science*, vol. 288, pp. 494–497, 2000.

[18] D. C. Hansen, K. M. Hansen, T. L. Ferrell, and T. Thundat, "Discerning Biomolecular Interactions Using Kelvin Probe Technology," *Langmuir*, vol. 19, pp. 7514–7520, 2003.

[19] M. Thompson, L.-E. Cheran, M. Zhang, M. Chacko, H. Huo, and S. Sadeghi, "Label-free Detection of Nucleic Acid and Protein Microarrays by Scanning Kelvin Nanoprobe," *Biosens. Bioelectron*., vol. 20, pp. 1470–1481, 2005.

[20] Mingquan Zhang, "Label-free Detection of Oligonucleotide Microarrays by the Scanning Kelvin Nanoprobe," Ph.D. dissertation, Dept. of Chemistry, Univ. of Toronto, 2008.

Jin-Hong Ahn received the B.S. and M.S. degrees in electronic engineering from Seoul National University in 1982 and 1984, respectively. He was with LG Semiconductor from 1984 to 1999 as a Memory design engineer, and Hynix Semiconductor from 1999 to 2008 as a research fellow of advanced DRAM design. Since 2008, he has been with Nano Systems Institute (NSI) in Seoul National University as a principal researcher. His research areas in NSI are electrical sensors using nano materials and array type biosensor chip design for medical applications.

Seok Hyang Kim received the B.S., M.S., degree in electronic engineering from Seoul National University, Seoul, Korea, in 2008, 2010, respectively. He is currently working toward the Ph.D. degree in electrical engineering and computer science at Seoul National University.

Jaeheung Lim received the B.S. degree in electronic engineering from Seoul National University, Seoul, Korea, in 2008. He is currently working toward the Ph.D. degree in electrical engineering and computer science at Seoul National University.

JungWoo Ko received the B.S. degree at Jeju National University, M.S. and Ph.D. degrees at Seoul National University, Korea in 1997, 2000, and 2007, respectively. He was with the Nano Systems Institute, Seoul National University, from 2007 to 2011. Since 2011, he has been with the Technology Commercialization Support Team, Electronics and Telecommunications Research Institute, Korea.

Chan Hyeong Park received the B.S., M.S., and Ph.D. degrees in electronics engineering from Seoul National University, Seoul, Korea, in 1992, 1994, and 2000, respectively. From 2000 to 2003, and from 2009 to 2012 he was a Visiting Scientist and a Visiting Professor, respectively with the Research Laboratory of Electronics, Massachusetts Institute of Technology (MIT), Cambridge. Since 2003, he has been with Kwangwoon University, Seoul, where he is currently a Full Professor with the Department of Electronics and Communications Engineering, His current research interests include the modeling of semiconductor devices and biosensors.

Young June Park received the B.S. and M.S. degrees in electrical engineering from Seoul National University, in 1975 and 1977. He received the Ph.D. degrees in electrical engineering from University of Massachusetts, USA, in 1983. From 1983 to 1988, he worked for IBM, East Fishkill, NY, and LG Semiconductor, Seoul, as a research staff member. In 1988, he joined Seoul National University as a faculty member and has contributed to education, semiconductor lab establishment, consulting to companies (as the R&D director in SK Hynix) and government of Korea. His research areas of interest include the nano semiconductor device physics, reliability, bio molecular sensing using semiconductor devices.